

—研究論文—  
Scientific Paper

## Equatorial electrojet dependence on solar activity in the Southeast Asia sector

Nurul Shazana Abdul Hamid<sup>1,2\*</sup>, Huixin Liu<sup>3,4</sup>, Teiji Uozumi<sup>4</sup>  
and Kiyohumi Yumoto<sup>3,4</sup>

東南アジア地域における赤道ジェット電流の太陽活動依存性

Nurul Shazana Abdul Hamid<sup>1,2\*</sup> · Huixin Liu<sup>3,4</sup> · 魚住禎司<sup>4</sup> · 湯元清文<sup>3,4</sup>

(Received December 17, 2012; Accepted April 19, 2013)

**要旨:** 赤道ジェット電流 (equatorial electrojet: EEJ) は、昼側磁気赤道直下における電離層電気伝導度の局所的増強に起因する電流系である。我々は、波長 10.7 cm の太陽電波強度 (F10.7) を太陽活動度の指標として用いて、EEJ強度の太陽活動度依存性を調査した。本研究で我々は、MAGDAS/CPMN 観測網のデータを用いて新しく構築された EEJ 指数の一つの成分である *EUEL* 指数のうち、2011 年の東南アジア地域のデータから算出された *EUEL* 指数を解析に用いた。磁気赤道から  $\pm 3^\circ$  の狭い緯度帯に集中して流れる EEJ 帯の内側と外側にそれぞれ位置する 2 観測点で得られた *EUEL* 指数の差から EEJ 強度を算出し (2 観測点法)、F10.7 強度と EEJ 強度に関してパワースペクトル解析と相関解析を行った。その結果、F10.7 変動と正相と同期した約 24 日と 28 日周期を持つ EEJ 強度の変動成分の存在を見いだした。一方で EEJ 強度の日変化は、解析を行った期間、F10.7 の日変化と、低い相関を示していたことが明らかとなった。

**Abstract:** The equatorial electrojet (EEJ) is a current system caused by the enhanced ionospheric conductivity near the dayside magnetic dip equator. We examined the dependence of the EEJ on solar activity, represented by the 10.7 cm solar radio flux (F10.7). For this analysis, we used a new equatorial electrojet index, *EUEL*, provided by the MAGDAS/CPMN network in the Southeast Asia sector for the year 2011. Using a two-station method, the EEJ strength was calculated as the difference between the *EUEL* index of the dip equator station and the *EUEL* index of the off-dip equator station located outside the narrow channel ( $\pm 3^\circ$  in latitudinal range) of the EEJ band. The relationship between the EEJ component and the F10.7 index was then examined using power spectrum and correlation analyses. We found approximate 24-day and 28-day periodicities in the EEJ

<sup>1</sup> 九州大学大学院理学府地球惑星科学専攻. Department of Earth and Planetary Sciences, Graduate School of Sciences, 33 Kyushu University, 6-10-1 Hakozaki, Higashi-ku, Fukuoka 812-8581.

<sup>2</sup> School of Applied Physics, Faculty of Science and Technology, Universiti Kebangsaan Malaysia, 43600 UKM, Bangi, Selangor, Malaysia.

<sup>3</sup> 九州大学大学院理学府地球惑星科学部門. Department of Earth and Planetary Sciences, Faculty of Sciences, 33 Kyushu University, 6-10-1 Hakozaki, Higashi-ku, Fukuoka 812-8581.

<sup>4</sup> 九州大学国際宇宙天気科学・教育センター. International Center for Space Weather Science and Education (ICSWSE), Kyushu University 53, 6-10-1 Hakozaki, Higashi-ku, Fukuoka 812-8581.

\* Corresponding author. E-mail: shazana.ukm@gmail.com

component, which are in phase with F10.7 variations. On the other hand, the daily values of EEJ showed low correlation with the daily F10.7 variations during the study period.

## 1. Introduction

The abnormally large amplitude of the horizontal geomagnetic field component measured at the magnetic equator is caused by the intense current flowing in the equatorial ionosphere. In the dayside equatorial ionosphere, the combination of the eastward electric field,  $\underline{E}_y$ , generated by the global dynamo with the northward magnetic field,  $\underline{B}$ , results in an eastward Pedersen current and downward Hall current. Here, the Hall current is less than 25% of the Pedersen current density. This Hall current leads to an accumulation of charges at the edges of dynamo layer, which results in the formation of an upward polarized electric field,  $\underline{E}_H$ . The magnitude of  $\underline{E}_H$  is about 20 times that of  $\underline{E}_y$ . This field continues to increase in strength until its own Pedersen current compensates the downward Hall current. The field also produces its own Hall current that flows in the eastward direction. The primary Pedersen current,

$$\underline{j}_p = \sigma_1 \underline{E}_y,$$

is in response to the peak Pedersen conductivity at about 130 km altitude, whereas the secondary Hall current,

$$\underline{j}_H = \sigma_2 \underline{B} \times \underline{E}_H / B,$$

is in response to the peak Hall conductivity near 110 km altitude (Onwumechili, 1997; Prölss, 2004). This is consistent with rocket observations which showed that the lower current layer peaks at an altitude of  $107 \pm 2$  km and the upper current layer peaks at  $136 \pm 8$  km (Onwumechili, 1992 a). The intense lower current layer, flowing eastward near the equator, is defined as the equatorial electrojet (EEJ), whereas the weak upper current layer is suggested to be part of the global Sq current that is driven by the global wind dynamo, which is eastward on the equatorial side of the Sq focus and westward on its polar side (Onwumechili, 1992 b). Because the lower layer current consists of mainly the secondary Hall current and the upper layer current consists of mainly the primary Pedersen current, the EEJ practically corresponds to  $\underline{j}_H$  while Sq at the equator corresponds to  $\underline{j}_p$ . Both currents overlap at the magnetic equator to give

$$\underline{j}_T = \underline{j}_p + \underline{j}_H = (\sigma_2^2 / \sigma_1 + \sigma_1) \underline{E}_y = \sigma_3 \underline{E}_y$$

where  $\sigma_3$  is known as Cowling conductivity (Hirono, 1950, 1952). Detailed studies of these currents have been reported by Forbes (1981) and Stening (1995). The ground magnetometer observations at the equator are directly influenced by  $\underline{j}_T$ . There are two schools of thought regarding the definition of EEJ: one defines the EEJ as the enhanced part ( $\underline{j}_H$ ) of the current at the equator in comparison to low latitudes, and the other defines the EEJ as the total current  $\underline{j}_T$  that includes the Sq contribution. On the basis of the physics of the equatorial current formation described above, we adopt the first definition here. As an independent current system, the EEJ has its own return current that differs from those of the

global Sq system. Beyond the flanks of the dip equator at about  $3^\circ$ , a downward electric field,  $\underline{E}_L$ , dominates and consequently the EEJ current,  $\sigma_2 \underline{E}_L$ , reverses and flows westward; this is the return current of the EEJ (Onwumechili, 1992 b). The EEJ return current is weak and covers a much greater latitudinal range than the forward current. In all ground-based and satellite profiles, the EEJ current is fully returned below the  $30^\circ$  dip latitude, on the equatorial side of the Sq focus. Therefore, the observed ground magnetic field at low latitude is not only a result to the Sq current, but is due to both the Sq current and the EEJ return current. However, the EEJ return current is much less intense than the global Sq current and therefore the effect of this current on magnetic measurement in low latitude regions is small compared to the Sq current.

Both the Sq and EEJ current intensities can vary on different time scales. Some previous studies have briefly discussed the relation of Sq and EEJ currents to solar activity. Briggs (1984) proposed a clear 27-day periodicity for the Sq fields, which was in phase with the variations in solar 10.7 cm (a frequency of 2.8 GHz) radio flux, abbreviated F10.7. This index is a general indicator of solar activity and has often been used as a proxy for solar extreme ultraviolet (EUV) radiation (Huang *et al.*, 2009). The influences of solar activity on the EEJ intensity and density were discussed by Rastogi *et al.* (1994) and Onwumechili (1997), respectively. Uozumi *et al.* (2008) detected the same dominant peak in both the power spectrum of F10.7 and of the  $H$  component at a station near the dip equator using a new EE-index. Recently, using the second definition of EEJ (Sq contribution is included), Yamazaki *et al.* (2010) demonstrated that EEJ intensity correlated to F10.7 variations with a sensitivity of  $77 \pm 12$ . They defined the EEJ sensitivity to F10.7 as  $(b/a) \times 10^4$  using least-square regression in the form of

$$EEJ = a + b \times F10.7.$$

The present study uses a new *EUEL* index derived from the Magnetic Data Acquisition System (MAGDAS) in the Circum-pacific Magnetometer Network (CPMN) (Yumoto and the CPMN Group, 2001). The aim of this study is to clarify the dependence of EEJ components on the solar activity represented by the F10.7 index extracted from the NASA Goddard Space Flight Center's OMNI data set through OMNI Web (<http://omniweb.gsfc.nasa.gov/>). Most former studies of the relation between the EEJ and solar F10.7 flux have limited their analyses to quiet day periods. In this study, we used a new approach and analyzed long and continuous data rather than data for selected quiet days. In the following section, we describe the *EUEL* index used in this study and the data processing methods. We then present the results of our spectrum and correlation analyses followed by the implications of findings with reference to previous publications.

## 2. Data and analysis

Close to the dip equator, the EEJ and the global Sq current interact and overlap. In order to isolate the EEJ component, we subtract the possible contributions of the global Sq current to the magnetometer measurements using a two-station method, assuming that the Sq component at the station located a few degrees away from equator is the same as the Sq component that overlaps with the EEJ at the magnetic equator station. Table 1 provides

Table 1. Geographic and Geomagnetic Coordinate of observatories stations used in this study.

Station Name	Code	GG Lat. (°)	GG Lon. (°)	GM Lat. (°)	GM Lon. (°)
Davao	DAV	7	125.4	-1.02	196.54
Muntinlupa	MUT	14.37	121.02	6.79	192.25

details of the Southeast Asia sector stations that were used in this study. The pair consists of Davao (DAV) Station which is located at the EEJ footprint (dip equator) and Muntinlupa (MUT) Station which is located outside the EEJ band (off-dip equator). Both stations have similar geomagnetic longitudes. Analysis is performed using data for 2011, a year in which the solar cycle was in an inclining phase.

The traditional method of calculating the EEJ strength involves obtaining the EEJ from the horizontal intensity on quiet days as  $\Delta H_{dip\ equator} - \Delta H_{off-dip\ equator}$ , where  $\Delta H$  is the variation in  $H$  from the mean midnight level for that observatory (Yacob, 1977; Manoj *et al.*, 2006). For this study, we use a new electrojet index named the *EUEL* index. To construct the *EUEL* index, the median value of the geomagnetic northward,  $H$ , component data was first subtracted from the original magnetic data to obtain  $ER_S$  for each available equatorial station,  $S$ . The relative magnetic variation of  $ER_S$  corresponding to  $\Delta H$  as the median value can be used to estimate the non-disturbed nighttime ambient level. Next, the mean value of  $ER_S$  observed at the nightside (LT = 18–06) MAGDAS/CPMN stations along the magnetic equatorial region, defined as  $EDst$ , is subtracted from the  $ER_S$  data of each equatorial station to compute the *EUEL* index. The  $EDst$  (equatorial disturbance in storm time) index has been found to show variations similar to the  $Dst$  index. The  $EDst$  index represents the global magnetic variation, including disturbances in the equatorial region (particularly from sudden storm commencement [SSC] or Chapman-Ferraro and ring current) and part of disturbances of magnetospheric origin such as substorms and the DP2 effect. For the off-dip equator station, we consider the latitudinal disturbance variation by subtracting  $EDst^* \cos(\phi)$ , where  $\phi$  is the geomagnetic latitude of the station. Thus, the disturbance effects of SSC and ring currents and some disturbances of magnetosphere origin are removed from the *EUEL* index, allowing us to analyze the continuous data set. For details of the creation of these indices, see Uozumi *et al.* (2008).

The magnetic EEJ component was determined as follows. For each station, the hourly magnetic EEJ component is calculated as

$$\Delta EUEL = EUEL_{dip\ equator} - EUEL_{off-dip\ equator}$$

Occasionally, the normal EEJ current reverses in the westward direction, a phenomenon called the counter electrojet (CEJ). The CEJ is observed as a depression in the horizontal intensity measured in the equatorial regions. It occurs mainly a few hours after dawn and a few hours before dusk but is rarely observed around local noon. Rastogi and Iyer (1976) showed that the EEJ strength reached its maximum around 1100 LT during solar minima and around 1200 LT during solar maxima. Thus, by using data around noontime, we limit our analysis to the period in which the EEJ current is strongest and can ignore the morning and evening effects. The daily EEJ in this study is obtained by taking the maximum  $\Delta EUEL$  value between 1000 and 1400 LT, as illustrated in Fig. 1.

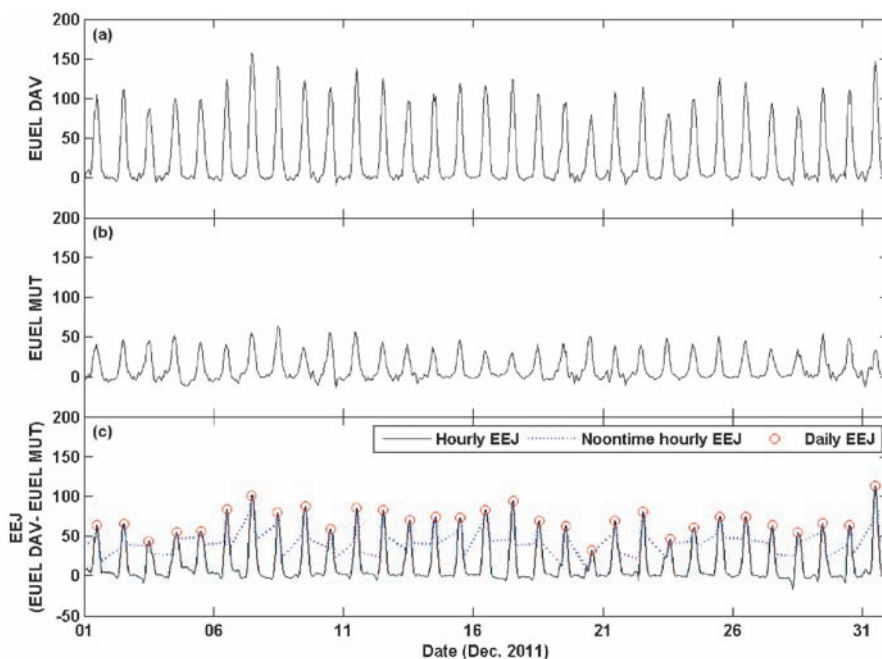


Fig. 1. Data processing of EEJ component. Hourly EEJ is obtained by (a) hourly EUEL from DAV subtract (b) hourly EUEL from MUT. (c) Daily EEJ (circle marker) is given by the maximum hourly EEJ during noontime.

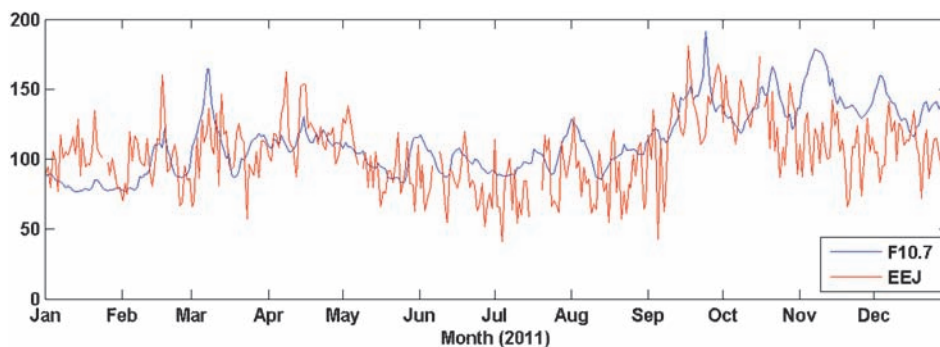


Fig. 2. Daily F10.7 and daily EEJ during a year of 2011.

### 3. Results and discussion

Figure 2 shows the obtained daily EEJ component together with the daily F10.7 used in the analysis. In this figure, the EEJ plot was graphically shifted upward. The F10.7 flux values during the year 2011 are mostly in the range of 80–150 sfu ( $1 \text{ sfu} = 10^{-22} \text{ W m}^{-2} \text{ Hz}^{-1}$ ) unlike during high solar activity years which commonly have values between 150 and 200 sfu. The F10.7 values began to increase by the end of the year with a possible

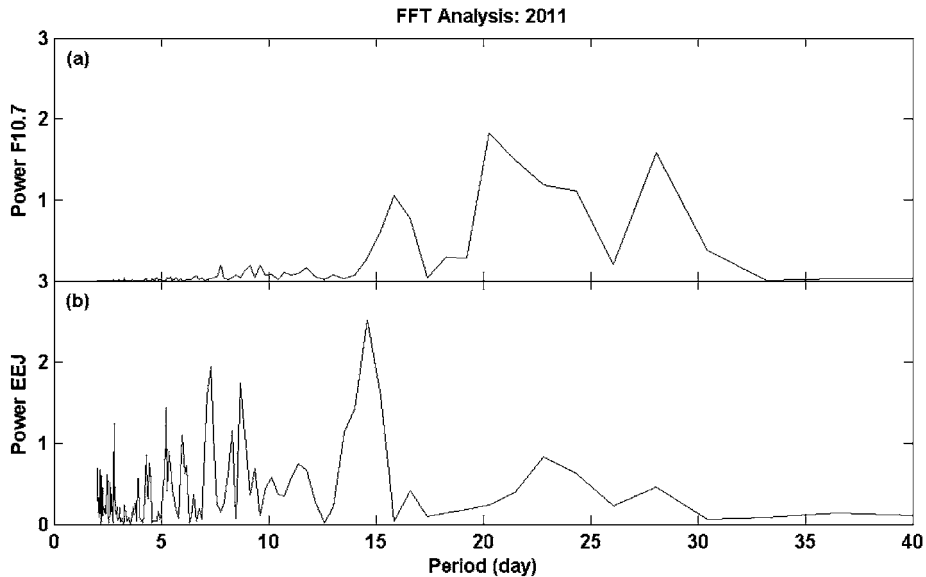


Fig. 3. Power spectrum of (a) F10.7 and (b) EEJ component obtained from DAV-MUT Station pair during a year of 2011.

periodicity of 27-day solar rotation. This clearly demonstrates that during the study period the solar cycle was in the inclining phase. From these superimposed plots, we can also see that both the F10.7 and EEJ data follow a similar trend.

Figure 3 shows the power spectrums of daily F10.7 and daily EEJ obtained from the DAV-MUT Station pair. Several dominant peaks appear in both spectrums. Two dominant 20-day and 28-day peaks appear in the F10.7 power spectrum. The EEJ shows a predominant peak at 14.5 days, which is similar to the 14-day periodicity of lunar origin (Forbes, 1981). Other dominant peaks appear around 24 and 28 days in the EEJ spectrum and may correspond to the peaks that appear in the F10.7 spectrum.

To confirm this relation, we conducted a cross spectrum analysis between daily F10.7 and daily EEJ. Cross spectrum analysis indicates the relationship between two time series at a certain frequency or period. Two aspects of such analysis are the coherence spectrum and phase spectrum. The coherence spectrum provides a measure of the stochastic coupling of the two signals within a certain frequency band, with values ranging from 0 (uncorrelated) to 1 (perfectly correlated). This function can show the frequencies at which two sets of time-series data are coherent or incoherent. The phase spectrum measures the phase shift between the data sets at each frequency. The result is shown in Fig. 4. Similar to power spectrums, peaks appear at approximately 24 and 28 days in the cross spectrum between F10.7 and EEJ. At these peaks, the coherence reaches values of 0.9858 and 0.9993, respectively, with a phase difference of nearly zero.

We then quantified this relationship by using correlation analysis. In contrast to the coherence function, the correlation coefficient describes both the direction (positive or negative) and degree (strength) of relationship between two signals over a certain time with values varying from  $-1$  to  $1$ . We present the results of both auto-correlation and cross-

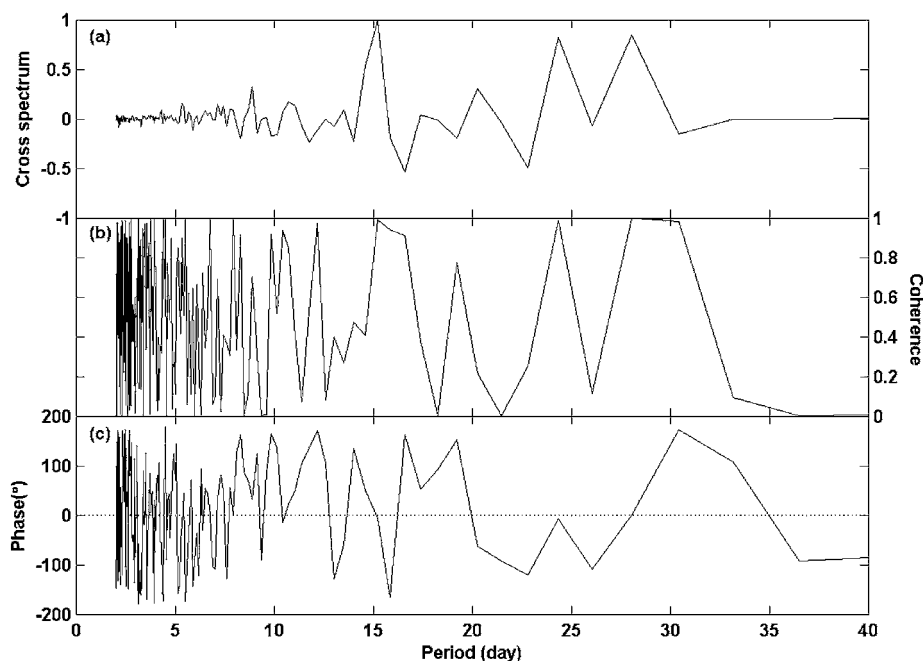


Fig. 4. (a) Cross spectrum, (b) coherence and (c) phase angle between daily F10.7 and daily EEJ.

correlation analyses in Fig. 5. The temporal day-to-day variations of both auto-correlations of F10.7 (Fig. 5 a) and EEJ DAV (Fig. 5 b) have a similar pattern. The peak at 20 days at both sides of time lag is present in the F10.7 auto-correlation but not in the EEJ auto-correlation. These peaks correspond to the 20-day peak in the power spectrum of F10.7 that can be seen in Fig. 3. The cross-correlation between F10.7 and the EEJ is displayed in Fig. 5 c. The correlation coefficient between F10.7 and the EEJ at zero lag was found to be 0.45, which indicates that EEJ current does not fully correlate with the solar flux data, suggesting that the EEJ strength is influenced by other factors. A closer examination of the EEJ auto-correlation shows 5-day to 7-day peaks, which may indicate variations driven by the lower atmosphere. Because the *EDst* index contains only partial information on magnetosphere origin disturbance, its subtraction from the *EUEL* index may not fully eliminate the effects of magnetosphere origin disturbance. This may be one of the factors that influences EEJ strength and consequently affects the correlation value obtained.

Our cross-correlation value was quite low compared to value of 0.53 obtained by Yamazaki *et al.* (2010) using the same dip equator station. One reason for this difference could be the different period used in their study. Yamazaki *et al.* (2010) used data during almost one solar cycle (1996–2005), whereas we used data only for 2011. Furthermore, they used the second definition of EEJ, which includes the Sq contribution, whereas we excluded the Sq contribution. Our correlation value between F10.7 and EEJ is slightly higher than the value of 0.40 obtained by Sripathi (2012) using data from the Indian sector during the year 2008. In addition to using data from a different year, the difference could have resulted from the fact that the EEJ magnetic signature is weaker over India than in the Southeast Asia sector (Doumouya *et al.*, 2003).

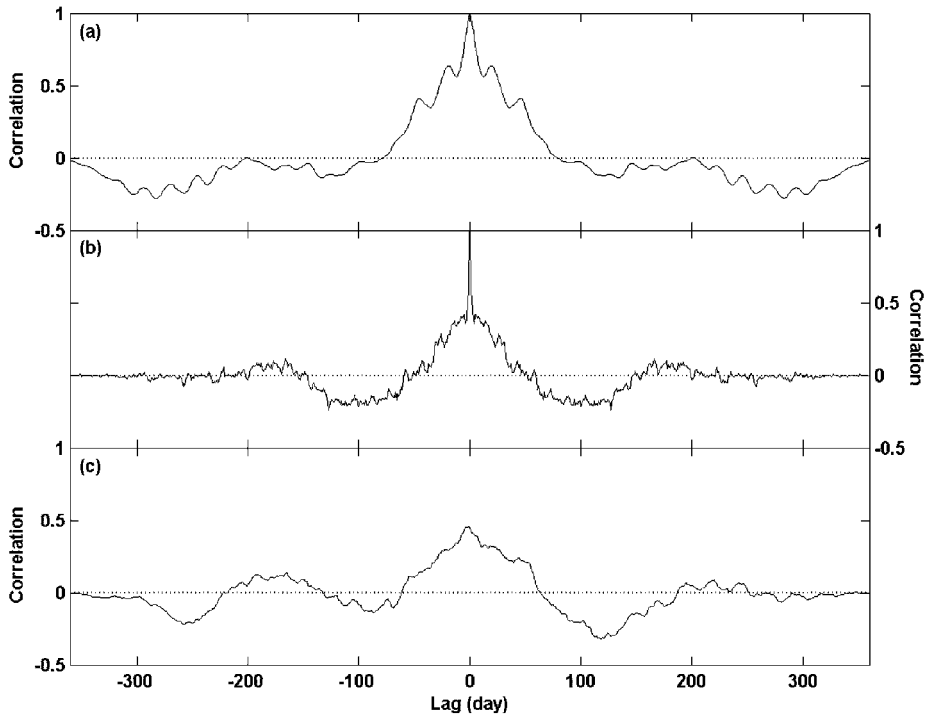


Fig. 5. Auto-correlation functions of the (a) daily F10.7 and (b) daily EEJ and (c) cross-correlation function between them.

#### 4. Summary

The solar F10.7 flux and the EEJ current represented by the *EUEL* index in the Southeast Asia sector during 2011 were found to have a similar trend. We performed both spectrum and correlation analyses to study the relationship between these indices. Our result confirms that F10.7 and the EEJ have higher coherence at periods of 24 and 28 days. This suggests that the solar flux has a significant impact on the EEJ strength at these time scales. Despite the higher coherence at these periods, both signals showed low correlation, likely owing to low coherence at other periods. The low correlation coefficient between the F10.7 and EEJ variations might indicate the influences of the lower atmosphere on the EEJ strength as well as magnetospheric disturbances. Because the magnetic signature of the EEJ strength is known to have a longitudinal dependence that is strongest in South America, moderate in West Africa, and lowest in Asia, analysis using data from other longitude sectors may provide a different result. Further research using data from different sectors and years will be performed in the near future to secure more accurate results.

#### Acknowledgements

The PI of the MAGDAS/CPMN project, Prof. Kiyohumi Yumoto, ICSWSE, Kyushu University, appreciates organizations and co-investigators around the world for their



cooperation and contribution to the MAGDAS/CPMN project. This work is supported by Japan Society for the Promotion of Science (JSPS) Core-to-Core Program, B. Asia-Africa Science Platforms. The work of H. Liu is supported by JSPS Grant-in-Aid for scientific research for young scientists (B) (No. 25800274). Financial supports were provided by JSPS as Grant-in-Aid for Overseas Scientific Survey (15253005, 18253005) and for publication of scientific research results (188068, 198055, 208043). The English in this document has been checked by at least two professional editors, both native speakers of English. For a certificate, please see: <http://www.textcheck.com/certificate/l5esI3>.

### References

- Briggs, B.H. (1984): The variability of ionospheric dynamo currents. *J. Atmos. Terr. Phys.*, **46**, 419–429, doi: 10.1016/0021-9169(84)90086-2.
- Doumouya, V., Cohen, Y., Arora, B.R. and Yumoto, K. (2003): Local time and longitude dependence of the equatorial electrojet magnetic effects. *J. Atmos. Sol.-Terr. Phys.*, **65**, 1265–1282, doi: 10.1016/j.jastp.2003.08.014.
- Forbes, J.M. (1981): The equatorial electrojet. *Rev. Geophys. Space Phys.*, **19**, 469–504, doi: 10.1029/RG019i003p00469.
- Hirono, M. (1950): On the influence of the Hall current to the electrical conductivity of the ionosphere. I. *J. Geomagn. Geoelectr.*, **2**, 1–8, doi: 10.5636/jgg.2.1.
- Hirono, M. (1952): A theory of diurnal magnetic variations in equatorial regions and conductivity of the ionosphere *E* region. *J. Geomagn. Geoelectr.*, **4**, 7–21, doi: 10.5636/jgg.4.7.
- Huang, C., Liu, D.D. and Wang, J.S. (2009): Forecast daily indices of solar activity, F10.7, using support vector regression method. *Res. Astron. Astrophys.*, **9**, 694–702.
- Manoj, C., Lühr, H., Maus, S. and Nagarajan, N. (2006): Evidence for short spatial correlation lengths of the noontime equatorial electrojet inferred from a comparison of satellite and ground magnetic data. *J. Geophys. Res.*, **111**, A11312, doi: 10.1029/2006JA011855.
- Onwumechili, C.A. (1992a): A study of rocket measurements of ionospheric currents-IV. Ionospheric currents in the transition zone and the overview of the study. *Geophys. J. Int.*, **108**, 660–672, doi: 10.1111/j.1365-246X.1992.tb04645x.
- Onwumechili, C.A. (1992b): Study of the return current of the equatorial electrojet. *J. Geomagn. Geoelectr.*, **44**, 1–42, doi: 10.5636/jgg.44.1.
- Onwumechili, C.A. (1997): *The Equatorial Electrojet*. Amsterdam, Gordon and Breach Science Publishers, 627 p.
- Prössl, G.W. (2004): *Physics of the Earth's Space Environment: an Introduction*. Berlin, Springer, 513 p.
- Rastogi, R.G. and Iyer, K.N. (1976): Quiet day variation of geomagnetic *H*-field at low latitudes. *J. Geomagn. Geoelectr.*, **28**, 461–479, doi: 10.5636/jgg.28.461.
- Rastogi, R.G., Alex, S. and Patil, A. (1994): Seasonal variations of geomagnetic *D*, *H* and *Z* fields at low latitudes. *J. Geomagn. Geoelectr.*, **46**, 115–126, doi: 10.5636/jgg.46.115.
- Sripathi, S. (2012): COSMIC observation of ionospheric density profiles over Indian region: ionospheric conditions during extremely low solar activity period. *Indian J. Radio Space*, **41**, 98–109.
- Stening, R.J. (1995): What drives the equatorial electrojet? *J. Atmos. Terr. Phys.*, **57**, 1117–1128, doi: 10.1016/0021-9169(94)00127-A.
- Uozumi, T., *et al.* (2008): A new index to monitor temporal and long-term variations of the equatorial electrojet by MAGDAS/CPMN real-time data: *EE-Index*. *Earth Planets Space*, **60**, 785–790.
- Yacob, A. (1977): Internal induction by the equatorial electrojet in India examined with surface and satellite geomagnetic observations. *J. Atmos. Terr. Phys.*, **39**, 601–606, doi: 10.1016/0021-9169(77)90070-8.
- Yamazaki, Y., Yumoto, K., Uozumi, T., Abe, S., Cardinal, M.G., McNamara, D., Marshall, R., Shevtsov, B.M. and Solov'yev, S.I. (2010): Reexamination of the *S<sub>q</sub>*-EEJ relationship based on extended magnetometer networks in the east Asian region. *J. Geophys. Res.*, **115**, A09319, doi: 10.1029/2010JA015339.
- Yumoto, K. and the CPMN Group (2001): Characteristics of Pi 2 magnetic pulsations observed at the CPMN stations: a review of the STEP results. *Earth Planets Space*, **53**, 981–992.